

H-Band dropouts in the deepest CANDELS fields

A new population of bright massive galaxies at $z > 3$

Belén Alcalde; Pérez-Gonzalez, Pablo; Barro, Guillermo; Eliche-Moral, Carmen; Dominguez, Helena; Esquej, Pilar

1. Motivation & objectives

The recent increase in depth, spatial and wavelength coverage of extragalactic surveys has improved dramatically our understanding of galaxies formation and evolution and is revealing a new population of galaxies at high redshift. That is consistent with a downsizing (Cowie et al. 1996, Heavens et al. 2004; Juneau et al. 2005; Bauer et al. 2005; Pérez-González et al. 2008) scenario, which implies that the most massive galaxies formed early in the history of the universe and evolved quickly. Thus, there should exist a population of massive passive evolving galaxies at those redshifts.

A small number of those death and red galaxies have already been spectroscopically or photometrically in recent works. Analyzing n-IR data allows us to detect sources that are very faint in optical wavelengths but bright in the n-IR (Thompson et al. 1999, Cimatti et al. 2002, Wilson et al. 2004). Their extremely red colors can be caused by either evolved stellar populations or very extinct starbursts. The analysis of their number density and properties is key ingredient to achieve a better understanding of evolution of galaxies during the first billion years of cosmic time.

In this context, we present preliminary results of our search for H-band dropouts: extremely red sources that are not detected in the deep HST WFC3 H-band but clearly detected in the two IRAC bluer bands in one of the most important cosmological fields: GOODS-N

3. Preliminary characterization of the sample

We search for counterparts of the sources in all available wavelength bands from the UV to the FIR. When the photometric data do not provides a constrained SED, we can derive any clear redshift estimation. For those sources, simple red color criteria are generally applied to photometry in the optical and IR bands to separate different types of galaxies and discriminate between those at high redshift and very dusty ones.

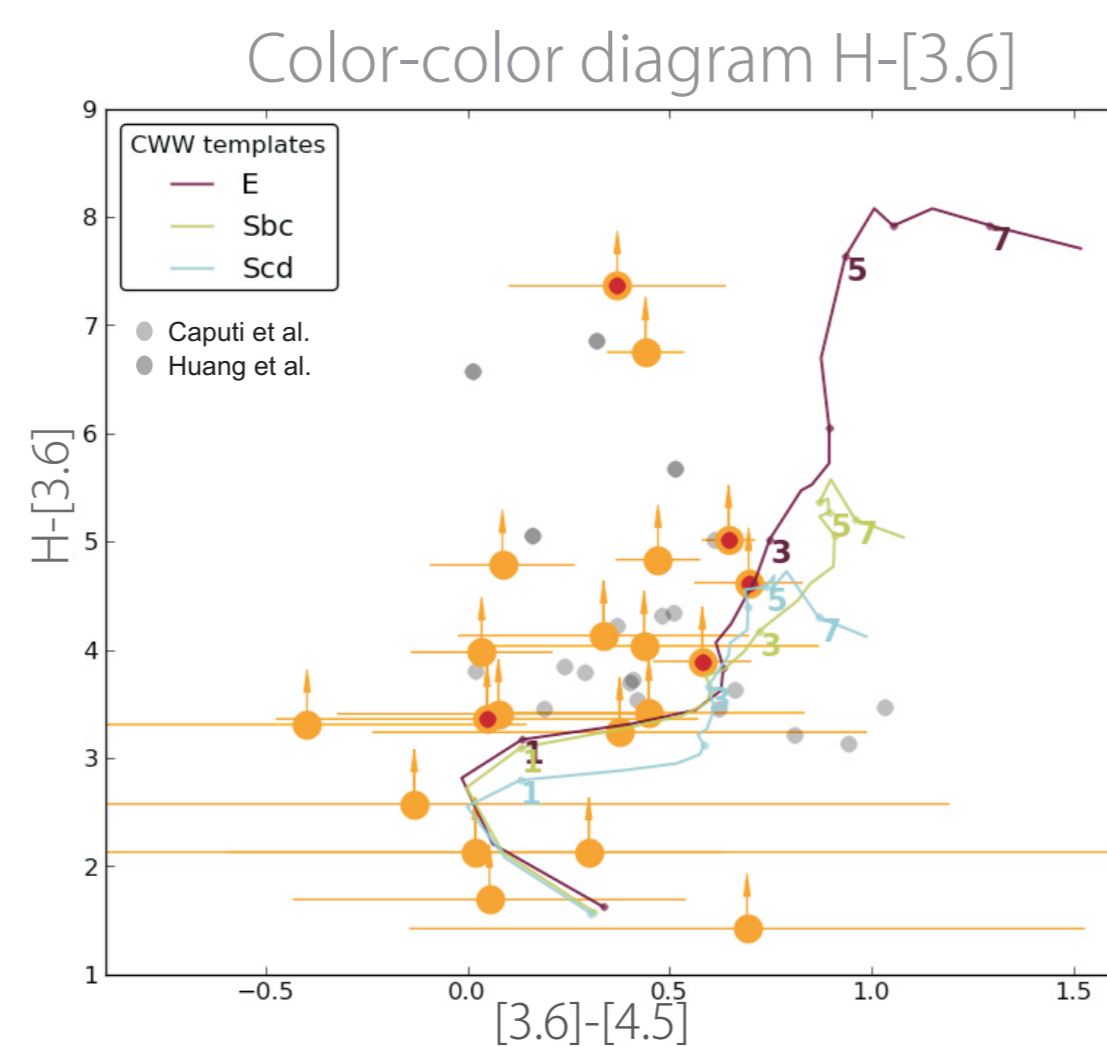
Color-selection criteria

Red color criteria and the analysis of deep mid-IR has been proved to be essential to constrain the presence of massive galaxies at $z \sim 5$ as shown in (Caputi et al. 2011 and Huang et al 2012).

The red colors of our sources are unlikely to be due to Lyman break with as it would imply $z > 10$. However, galaxies with a strong Balmer/4000Å break at $3 < z < 8$ can have very red H-[3.6] colors. It is very instructive to see the location of the sources in near-midIR color-color diagram especially for sources with unconstrained SED.

Being our candidates H-band dropouts we shouldn't have photometry from bluer bands. However, by forcing photometry we recover sources that weren't detected as they are in the detection limit.

Fig. Color-color diagram. Observed-frame H-[3.6] vs. [3.6] - [4.5] color-color diagram for all IRAC-selected galaxies in the GOODS-N (orange). Red dots indicate that those sources have a clear MIPS 24µm counterpart. Grey dots correspond to H-[3.6]>4.5 analyzed in Huang et al 2012 and H-[4.5]>4 reported in Caputi et al. 2012. We also present observed-frame color tracks for non-evolving E/S0, Scd SEDs (CWW E; Coleman et al. 1980).



Multiwavelength photometry & SEDs

For some sources, the multiwavelength photometry provides us a constrained SED that allows to derive more reliable redshifts and parameters. We present examples of our SED-fitting results. Both galaxies have an estimated redshift $z > 3$ and are detected in other bands. A, is characterized by a power-law spectrum while B is a very reliable detection. Can be classify as a $z_{phot} > 6$ galaxy that is best fitted by a power-law type template and is clearly detected in MIPS 24 while the other has $z_{phot} \sim 5$ and is clearly detected at mid-far IR including PACS & SPIRE.

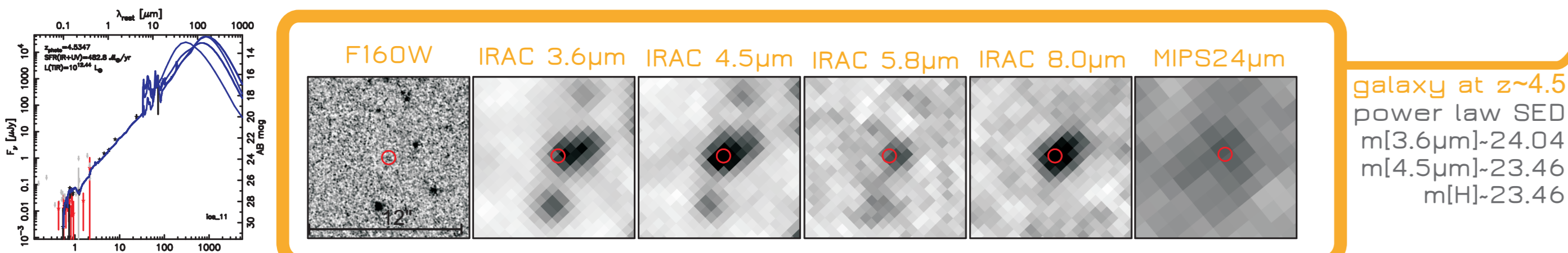
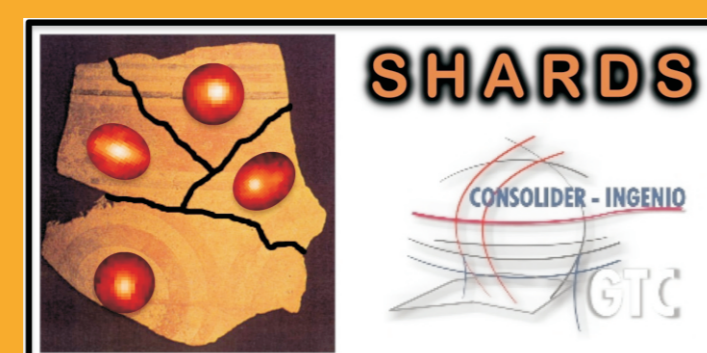


Fig. [Left] Results of best-SED fitting for a candidate with an estimated $z_{phot} \sim 4.5$, and presents a power-law spectrum. [Right] Postage stamps of the source in H-F160W, the four IRAC bands and MIPS 24µm. Each panel has a 12" width.

References

- Bauer et al. 2005
- Barro et al.
- Caputi et al. 2012
- Cimatti et al. 2002
- Cowie et al. 1996
- Daddi et al. 2009
- Haojing et al.
- Heavens et al. 2004
- Juneau et al. 2005
- J.-S. Huang et al.
- Laidder et al. 2007
- Pérez-González et al. 2008
- Thompson et al. 1999
- Wang et al. 2007
- Wilson et al. 2004



2. Image processing, selection process & photometry

Our **H-band dropouts sample**, has been built searching for extremely red objects in the Spitzer 3.6 and 4.5µm IRAC images that are not detected in the F160W CANDELS band over ~ 100 arcsec² of the GOODS-N field.

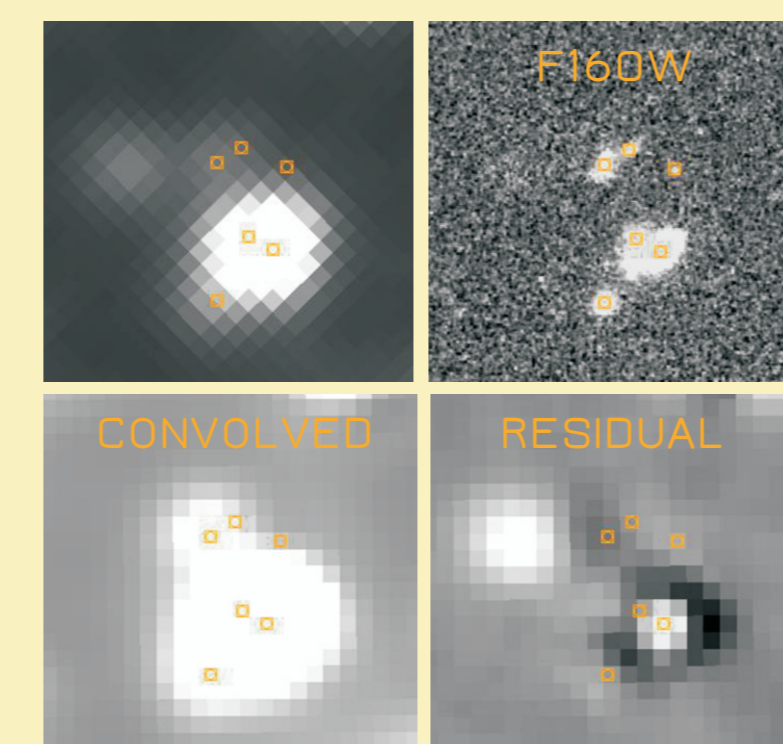


Fig. Example of deconvolution process of IRAC images from HST reference image.

The mIR images have very different and lower angular resolution ($\sim 2''$) than that obtained with the HST WFC3 H band ($\sim 0.2''$). A software package called TFIT (Laidder et al. 2007) is specially design to perform photometry given a high resolution and a low resolution image by using the spatial positions and morphologies of objects in the high resolution image to construct object templates, which are then fitted to the lower resolution image.

When **running TFIT** for IRAC images it produces an improved convolved image where the flux has to be scaled and also, after subtracting all the H-band detected galaxies, a residual image containing the remaining flux.

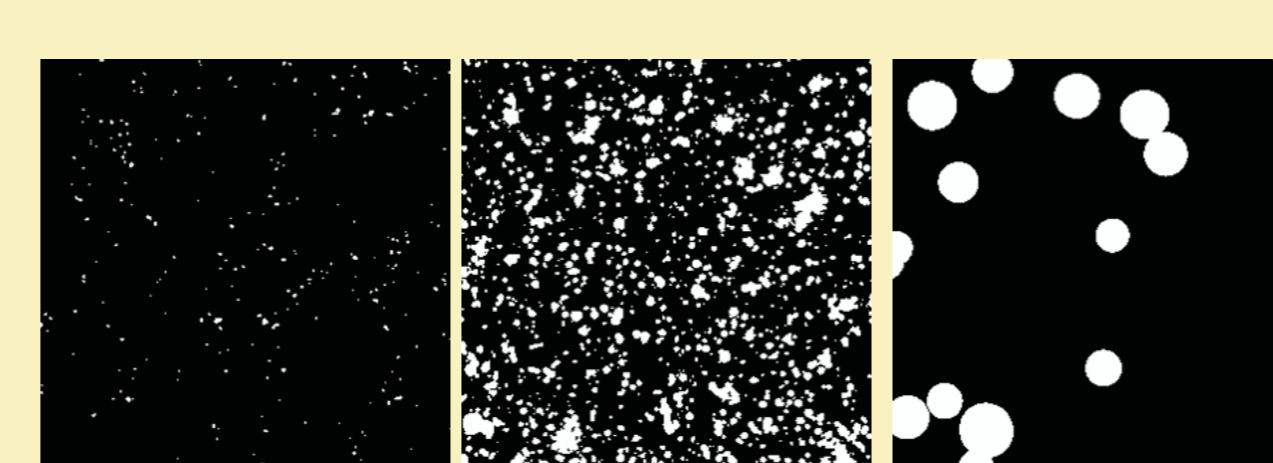
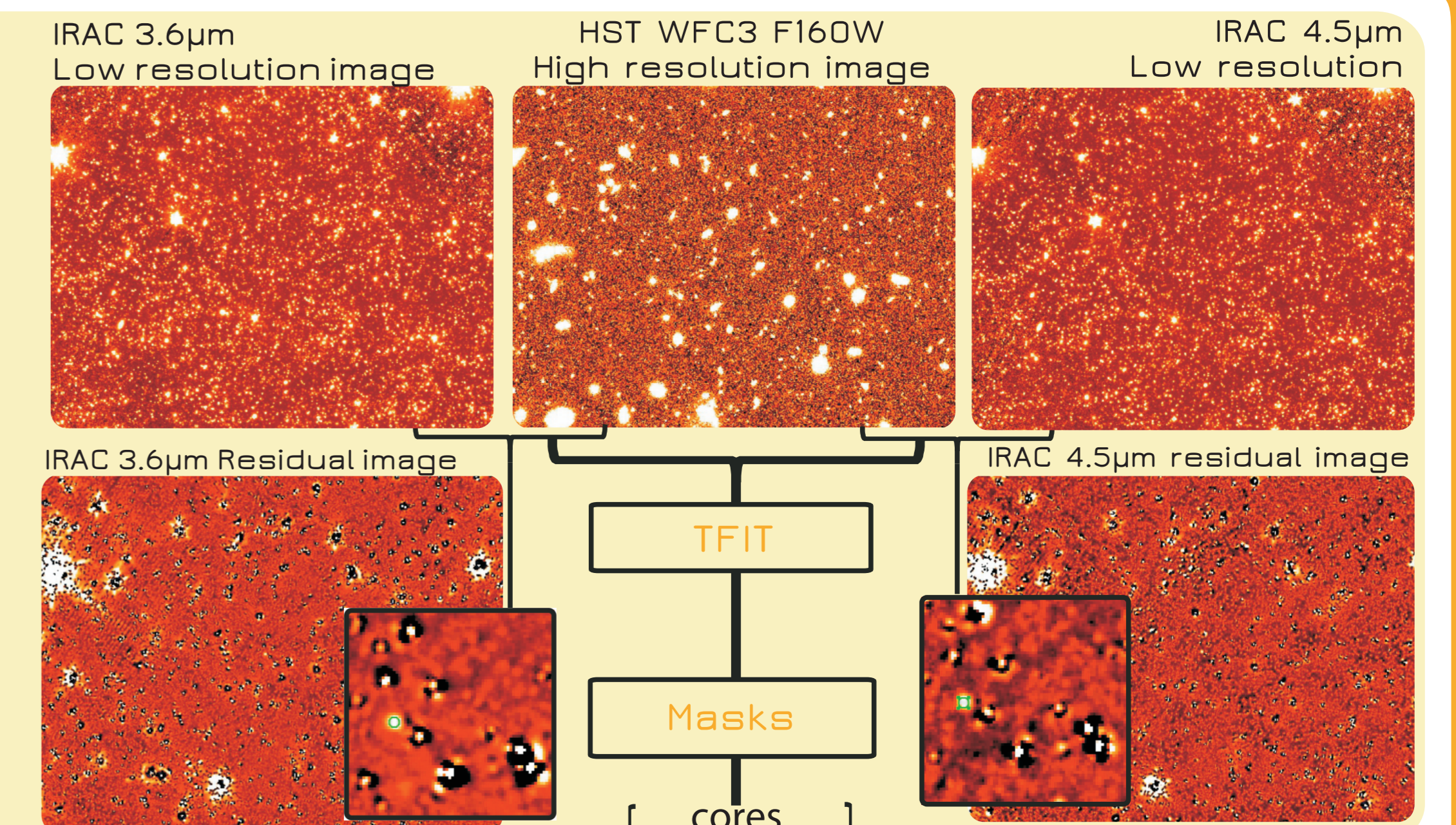
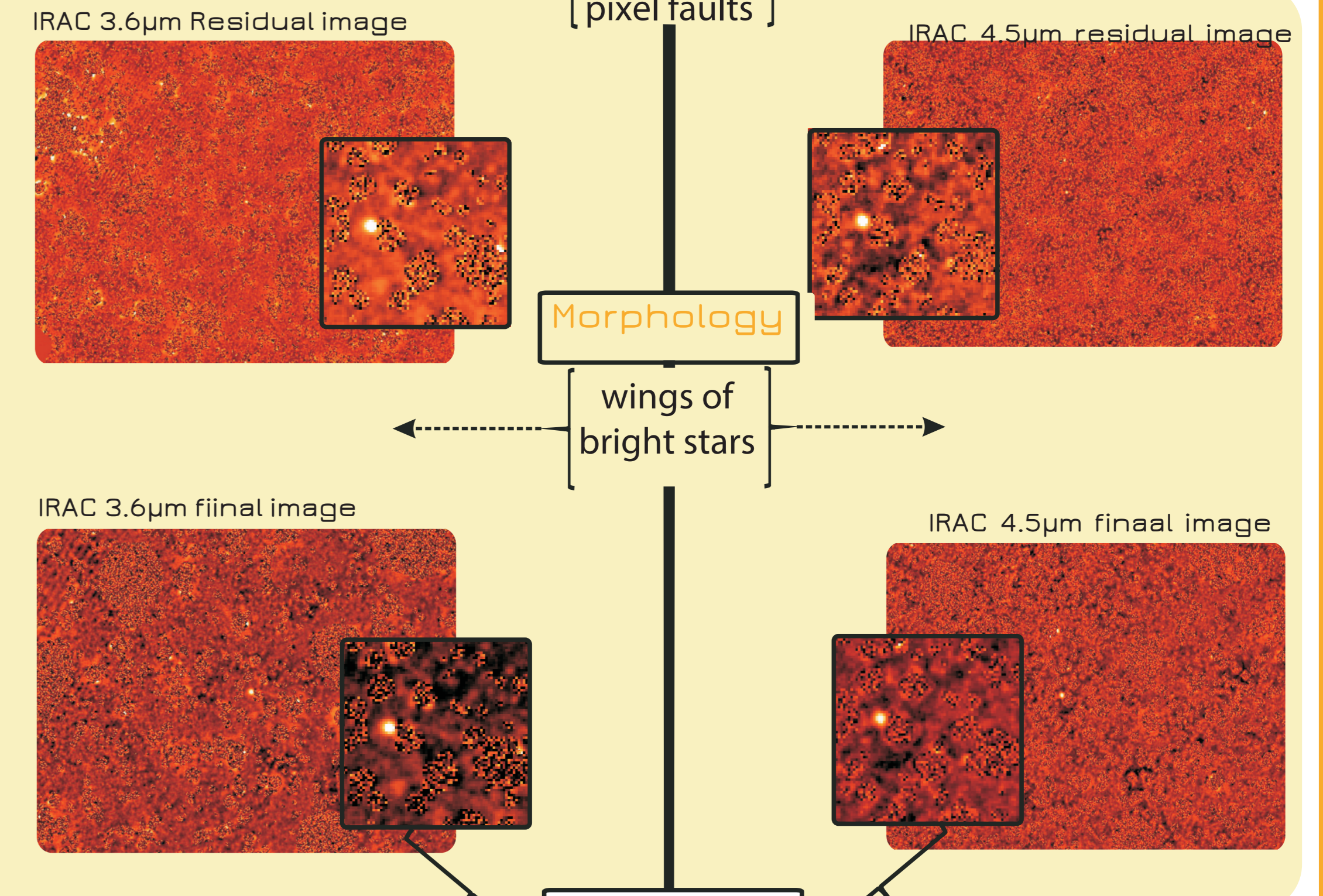


Fig. Masks applied to the residual IRAC images. The one on right include pixel faults, the one on the second mask cores from bright H-band sources and the one on the left is a mask for stars with $m < 20$ being the masked radio radio function of its magnitude

Thus, the flux from the H-band dropouts sources will remain in the residual images. However, those residual images do not only contain the galaxy candidates we are searching for but also remaining flux coming from the wings of bright sources. In order to avoid spurious detections, we clean the image prior to run SEXTRACTOR applying several masks.

First, we create a mask for pixels above a threshold flux, then we create another mask around the brightest ($m < 20$) stars in the field with a circular radio function of its magnitude and finally we mask fault pixels that appeared in the image during the convolution process.

All these **masks are applied to the residual image** and replaced by the median background with a gaussian noise. Next, we try to avoid detection of the remaining wings with **mathematical morphology** method.



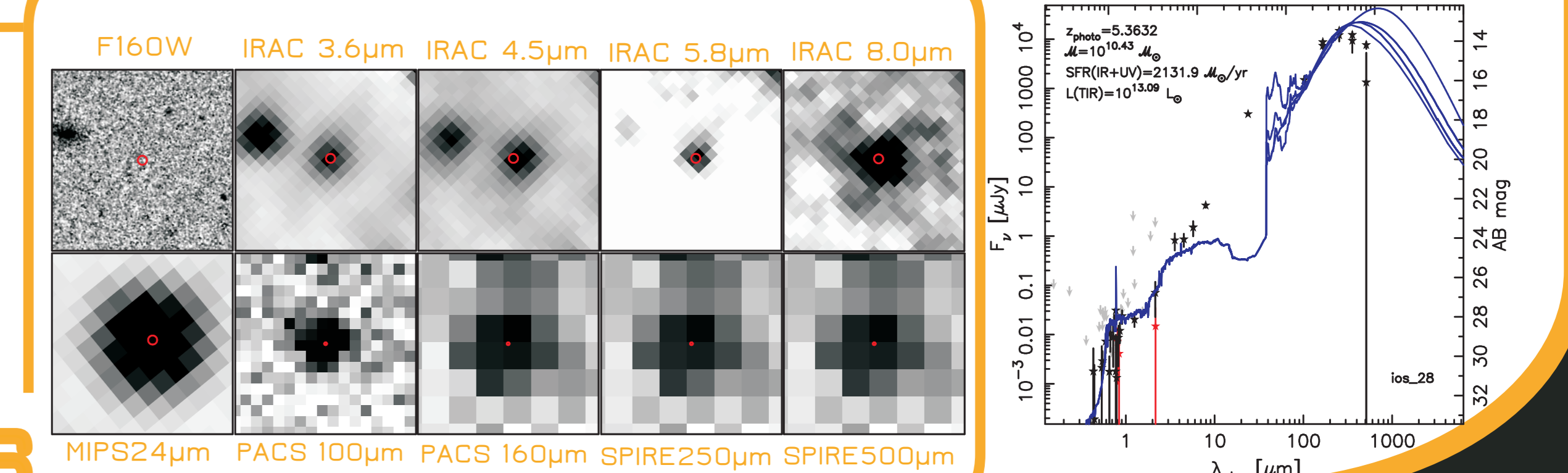
source detection

As we have followed the same procedure separately in 3.6 and 4.5µm we obtained two **different catalogues using SEXTRACTOR** in the two final images. To avoid spurious sources, we **cross-correlate** the catalogues and discard any source not detected in both.

Finally, we **visually inspect** the final images to remove any false source from our

galaxy at $z \sim 5.3$

Fig. [Left] Results of best-SED fitting for a candidate with an estimated $z_{phot} \sim 4.5$, and presents a power-law spectrum. [Right] Postage stamps of B; clearly detected in IRAC, MIPS, PACS and SPIRE. The panels of H-band, IRAC and MIPS have a 12" width but PACS and SPIRE ones have a 40" width.



bona fide H-band dropouts